HEFAT2012
9th International Conference on Heat Transfer, Fluid Mechanics and Thermodynamics
16 – 18 July 2012
Malta

MODELLING OF THE AIDING MIXED CONVECTION IN A VERTICAL RECTANGULAR CHANNEL

Poskas R.*, Zujus Re. and Gediminskas A.
*Author for correspondence
Nuclear Engineering Laboratory,
Lithuanian Energy Institute,
3 Breslaujos, LT-44403 Kaunas,
Lithuania,
E-mail: rposkas@mail.lei.lt

ABSTRACT

Many researchers have analyzed laminar and turbulent mixed convection in channel flows, however, despite their wide investigations, there are still many cases which are not well understood and difficult to predict. Investigations of heat transfer in the laminar-turbulent (transition) region under the effect of buoyancy (mixed convection) are rather limited. In this paper the results on numerical investigation of the local aiding mixed convection heat transfer in the laminar-turbulent (transition) region in a vertical rectangular channel are presented. Numerical 3D steady state simulations have been performed using Ansys Fluent code in air flow. Modelling has been performed using laminar and transitional (kkl-ω, SST and Re Stress ω) models. Modelling results demonstrate that vortexes exist in the central part of the channel. This makes velocity profiles asymmetrical. The results of numerical modeling have been compared with the results of experiments performed at the same conditions and previous results of 2D numerical modelling using laminar model.

INTRODUCTION

Mixed convection investigations (the interaction of the natural and forced convection) in channels of various cross-sections and orientations are important for nuclear power technology, heat exchangers, electronic cooling systems, solar energy systems, etc. Due to the importance of the engineering applications problem, a lot of researchers concentrated their attention on the turbulent mixed convection heat transfer investigations in vertical circular tubes [1 - 3]. Wide investigations on this problem (turbulent flow in vertical channels) were performed at the Lithuanian Energy Institute [4]. Different studies showed that compared to the forced convection, heat transfer was higher in case of the opposing mixed convection (upward oriented flow due to natural convection and downward oriented flow due to forced flow). It was revealed that in case of the aiding mixed convection flows (upward oriented flow due to natural convection and upward oriented flow due to forced flow), the effectiveness of heat transfer could be seriously impaired as a result of buoyancy forces modifying the production of turbulence and laminarizing the flow. However, if higher buoyancy parameters were applied, heat transfer recovered and became even higher than the forced convection heat transfer.

Investigations of heat transfer in the laminar-turbulent transition region under the effect of buoyancy (mixed convection) were rather limited.

NOMENCLATURE

b	[m]	Channel width
c_p	[J/kg K]	Specific heat
d_e	[m]	Equivalent diameter of the channel [$d_e = 2hb/(h+b)$]
Gr_q	[-]	Grashof number defined by the heat flux specified on the surface [$Gr_q = g \cdot \beta \cdot d_e^4 \cdot q_w / \nu^2 \cdot \lambda$]
g	[m/s^2]	Acceleration due to gravity
h	[m]	Channel height
i	[J/kg]	Enthalpy
Nu	[-]	Nusselt number [$Nu = \alpha d_e/\lambda$]
Pr	[-]	Prandtl number [$Pr = \mu c_p/\lambda$]
p	[Pa]	Pressure
q	[W/m^2]	Heat flux density
Re	[-]	Reynolds number [$Re = u d_e/\nu$]
u	[m/s]	Local flow velocity
x	[m]	Axial coordinate measured from start of heating
x, y, z	[m]	Coordinate
Special characters		
α	[W/m^{2}K]	Heat transfer coefficient
β	[1/K]	Volumetric expansion coefficient
λ	[W/mK]	Thermal conductivity
ν	[m^2/s]	Kinematics viscosity
μ	[Pa s]	Dynamic viscosity
ρ	[kg/m^3]	Density
Subscripts		
1, 2		First and second wall
in		At the inlet
w		At the wall
x, y, z		Coordinate

The flow character in pipes in this region was investigated in [5, 6]. In order to visualize the flow, paint was injected in the central part of the pipe. It was reported, that the shape of the paint thread in aiding mixed convection flows with the loss of flow stability was similar to the shape of sinusoid, and the pulsation of the temperature on the pipe's wall took its place. With the increase of the buoyancy parameter, the amplitude of the paint thread sinusoid became bigger, while eventually the paint thread intermitted at the end. The initial instability of the flow depended not only on the buoyancy parameter, but also on the length of the channel (L/d). In the case of the opposing mixed convection flows, the instability of the flow was demonstrated by the appearance of the asymmetry of the paint thread just before the heating. If the buoyancy parameter increased significantly, the flow began pulsating. It was noticed that an asymmetric flow was formed inside the channel. It was also noticed in [7, 8], that the existence of the flexure points in velocity profiles and especially the possibility of the appearance of the reversed flow, stimulated the loss of stability of laminar flow, as well as the transition to turbulent flow. The loss of stability and the transition to turbulent flow took place when $Re = Re_{cr} < 2.3 \cdot 10^3$. With the increase of Gr_q/Re, critical Reynolds number decreased. The correlation for calculation of the distance at which laminar flow loses its stability in case of the aiding mixed convection flows was suggested in [7]. In case of the opposing mixed convection flows with increasing Gr_q/Re, the flow became slower near the walls and in its core became faster. With $Gr_q/Re \approx 100$ velocity gradients became equal to zero near the wall, and with further increase of this parameter reversed flow appeared. When $Gr_q/Re \approx 170$ the instability took place, vortices appeared in the region near the wall, and then, under higher Gr_q/Re, the flow became turbulent.

The structure of the flow, in case of the opposing mixed convection, was studied in a vertical tube in [9] with moving thermocouples. After these investigations, it was concluded that at the beginning of the heating, vortices appear near the walls, which causes the fluctuation of wall temperature. As the influence of the buoyancy forces became stronger, the flow inside the channel became turbulent.

In [10] experiments (temperature and velocity fluctuations) in airflow for Re = 1000, 1300 and 1600 were performed. Flow instability in a vertical tube in case of the aiding mixed convection was analyzed. It was determined that flow lost its stability under Gr/Re > 1500.

In [11] the results on experimental and numerical investigation of the opposing mixed convection in a vertical flat channel with symmetrical heating in the laminar-turbulent transition region were presented. Numerical two-dimensional simulations were performed for the same conditions as in experiments using the Fluent code. The performed experimental investigations showed that for the higher than ambient air pressure in some Re region, heat transfer rate was more intensive than for the turbulent flow. The numerical investigations indicated that as the influence of the buoyancy became stronger, the vortical flows appeared at the wall of the channel, which caused the intensification of the heat transfer.

In this paper the results on numerical investigations of the local aiding mixed convection heat transfer in the laminar-turbulent transition region in the vertical flat channel are presented. Numerical three-dimensional (3D) simulations have been performed for the same channel and for the same conditions as in experiments using Ansys Fluent code. Simulations have been performed at air pressure p = 0.2 MPa with symmetrical heating for Reynolds numbers Re_{in} = 1300, 2000 and Grashof numbers $Gr_{qin} = 3.6 \cdot 10^8$, $3.8 \cdot 10^8$ accordingly.

METHODOLOGY

In this paper the results on three-dimensional numerical modelling of aiding mixed convection in the vertical rectangular channel (height – 0.0408 m, width – 0,4 m, length – 6 m, hydrodynamic unheated length – 2.5 m, heated (calorimeter) length 3.5 m) with two-sided symmetrical heating ($q_{w1} = q_{w2} = const$) are presented for the steady state flow conditions in airflow. The modelling has been performed using laminar and turbulence transition models: kkl-ω [12], SST [13, 14], and Reynolds Stress ω model [15, 16].

The modelling has been carried out using Ansys Fluent code. It is a contemporary computational fluid dynamics code which is used for modelling the fluid flow and heat transfer in complex two-dimensional or three-dimensional systems [17]. This code solves the main flow and energy equations. In this case a control volume based technique is used. It is based on division of the domain into discrete control volumes using a computational grid (which at the same time describes channel geometry).

The steady state mean flow equations to be solved in the three dimensional problem are these:

conservation of mass (continuity),

$$\frac{\partial(\rho u_x)}{\partial x} + \frac{\partial(\rho u_y)}{\partial y} + \frac{\partial(\rho u_z)}{\partial z} = 0 \qquad (1)$$

conservation of the u_x, u_y and u_z momentum,

$$\rho u_x \frac{\partial u_x}{\partial x} + \rho u_y \frac{\partial u_x}{\partial y} + \rho u_z \frac{\partial u_x}{\partial z} = -\frac{\partial p}{\partial x} + \\ + \frac{2}{3}\frac{\partial}{\partial x}\left[\mu\left(2\frac{\partial u_x}{\partial x} - \frac{\partial u_y}{\partial y} - \frac{\partial u_z}{\partial z}\right)\right] + \\ + \frac{\partial}{\partial y}\left[\mu\left(\frac{\partial u_x}{\partial y} + \frac{\partial u_y}{\partial x}\right)\right] + \frac{\partial}{\partial z}\left[\mu\left(\frac{\partial u_z}{\partial x} + \frac{\partial u_x}{\partial z}\right)\right] - \rho g_x \qquad (2)$$

$$\rho u_x \frac{\partial u_y}{\partial x} + \rho u_y \frac{\partial u_y}{\partial y} + \rho u_z \frac{\partial u_y}{\partial z} = -\frac{\partial p}{\partial y} + \\ + \frac{2}{3}\frac{\partial}{\partial y}\left[\mu\left(2\frac{\partial u_y}{\partial y} - \frac{\partial u_x}{\partial x} - \frac{\partial u_z}{\partial z}\right)\right] + \\ + \frac{\partial}{\partial z}\left[\mu\left(\frac{\partial u_y}{\partial z} + \frac{\partial u_z}{\partial y}\right)\right] + \frac{\partial}{\partial x}\left[\mu\left(\frac{\partial u_x}{\partial y} + \frac{\partial u_y}{\partial x}\right)\right] \qquad (3)$$

$$\rho u_x \frac{\partial u_z}{\partial x} + \rho u_y \frac{\partial u_z}{\partial y} + \rho u_z \frac{\partial u_z}{\partial z} = -\frac{\partial p}{\partial z} + \\ + \frac{2}{3}\frac{\partial}{\partial z}\left[\mu\left(2\frac{\partial u_z}{\partial z} - \frac{\partial u_x}{\partial x} - \frac{\partial u_y}{\partial y}\right)\right] + \\ + \frac{\partial}{\partial x}\left[\mu\left(\frac{\partial u_z}{\partial x} + \frac{\partial u_x}{\partial z}\right)\right] + \frac{\partial}{\partial y}\left[\mu\left(\frac{\partial u_y}{\partial z} + \frac{\partial u_z}{\partial y}\right)\right] \quad (4)$$

$$\rho u_x \frac{\partial i}{\partial x} + \rho u_y \frac{\partial i}{\partial y} + \rho u_z \frac{\partial i}{\partial z} = \frac{\partial}{\partial x}\left(\left(\frac{\mu}{\mathrm{Pr}}\right)\frac{\partial i}{\partial x}\right) + \\ + \frac{\partial}{\partial y}\left(\left(\frac{\mu}{\mathrm{Pr}}\right)\frac{\partial i}{\partial y}\right) + \frac{\partial}{\partial z}\left(\left(\frac{\mu}{\mathrm{Pr}}\right)\frac{\partial i}{\partial z}\right) \quad (5)$$

The transition SST model is based on the coupling of the SST k-ω transport equations [14] with two other transport equations, one for the intermittency and one for the transition onset criteria, in terms of momentum-thickness Reynolds number.

The transition kkl-ω model is considered to be a three-equation eddy-viscosity type model which includes transport equations for turbulent kinetic energy, laminar kinetic energy, and the inverse turbulent time scale.

The Re Stress ω model is a stress-transport model that is based on the k-ω equations [15] and LRR model [16].

Boundary conditions are:

- At the inlet to the channel longitudinal air velocity u_x is equal to inlet velocity u_{in}, transversal velocity $u_y = u_z = 0$. Air enthalpy i at the inlet to the calorimeter is equal to the inlet air enthalpy i_{in}.
- On the walls longitudinal u_x and transversal u_y, u_z velocities are equal to 0. Heat flux on the calorimeter walls (wide side walls) are $q_{w1} = q_{w2} = \text{const}$.

Grid convergence study (dependence of numerical accuracy on the spatial resolution) have been performed for $Re_{in} = 2000$. The comparison is made among two combinations of grid density interval (1000 × 20 × 75 and 800 × 20 × 60). It is shown that the numerical accuracy is nearly independent of grid density interval within their respective ranges tested. Therefore, the spatial 1000 × 20 × 75 resolution is adopted for all the cases studied. (**Figure 1**).

RESULTS

The numerical investigation has been performed for two Re numbers (Re_{in} = 1300, 2000). Results are very similar to each other, therefore more detailed analysis will be presented only for one Re number. The velocity profiles (3D and 2D transient modelling) for laminar model for Re_{in} = 1300 are illustrated in **Figure 2**.

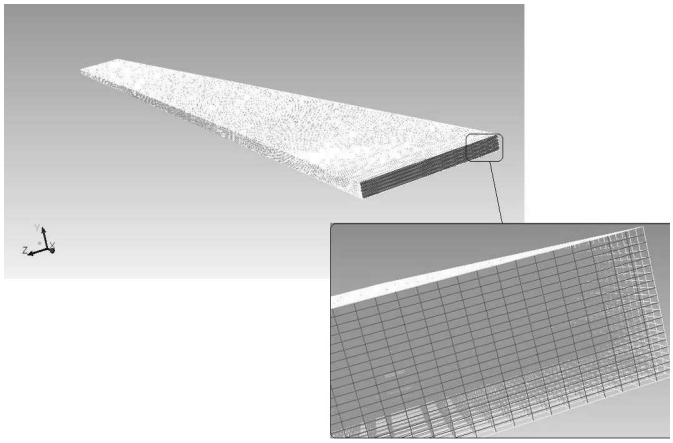

Figure 1 Computational domain and partial view of the grid

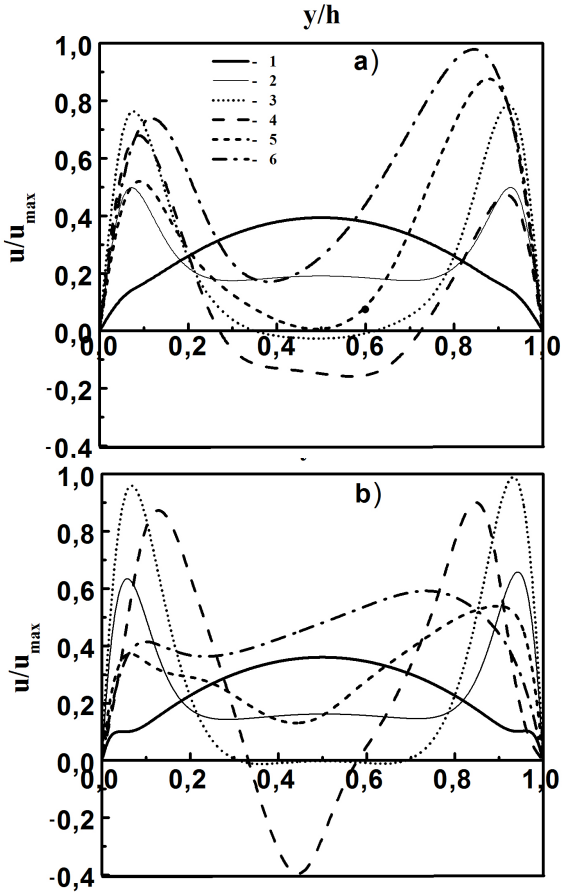

Figure 2 The dynamics of velocity profiles for Re_{in} = 1300, $Gr_{qin} = 3.6 \cdot 10^8$. a) 3D modelling; b) 2D modelling. 1 curve – x/d_e = 0.01; 2 – 2.7; 3 – 5.4; 4 – 8.1(b), 13.5(a); 5 – 13.5(b), 25.7(a); 6 – 42

When analyzing velocity profiles, flow developing processes can be observed. It is well known that the laminar flow has a parabolic velocity profile therefore, as the regime with such Re number is analyzed, in the hydrodynamic unheated part of the analyzed channel parabolic velocity profile

is forming. The upper part (in the centre) of such profile is also visible (**Figure 2** a, b) in the heated part of the analyzed channel at $x/d_e = 0.01$, but slight impact of natural convection is visible near the walls (near the walls velocity is increasing). With the increase of x/d_e, the velocity profile becomes typical to the aiding mixed convection flows i.e. near the walls velocity is higher than in the central part (M-shape velocity profile), and with increasing impact of the natural convection (for higher x/d_e), velocity is increasing near the channel walls. Moreover, in the central part at some x/d_e, velocity becomes negative and this means that reversal flow has appeared. Reversal flow is observed in some part of the channel, then vortexes intermit. The velocity profiles show that the reversed flow cannot be observed from $x/d_e \approx 26$ (in 3D case) and $x/d_e \approx 14$ (in 2D case).

Based on this information it can be stated that three-dimensional modelling results are similar to two-dimensional modelling results, because in both cases the vortical flow is observed, although vortexes remain longer along the channel in the three-dimensional case.

The flow structure that is presented below, gives additional information about the air flow in a rectangular channel for analyzed conditions.

When analyzing channel flow for fixed x/d_e (**Figure 3**), it can be seen that at the very beginning of the heated section ($x/d_e = 2.7$) there is only an impact of the unheated channel's wall i.e. near the unheated narrow side walls the velocity is smaller than in the central part. For larger x/d_e the velocity is slowing down in the central part of the channel and increasing near the heated wide side walls. There reversal flow is observed at $x/d_e = 13.5$. In the heat transfer stabilized region ($x/d_e = 42$) the flow structure is different. There are many small vortexes, and near the heated wide side walls of the channel the velocity is higher than in the central part.

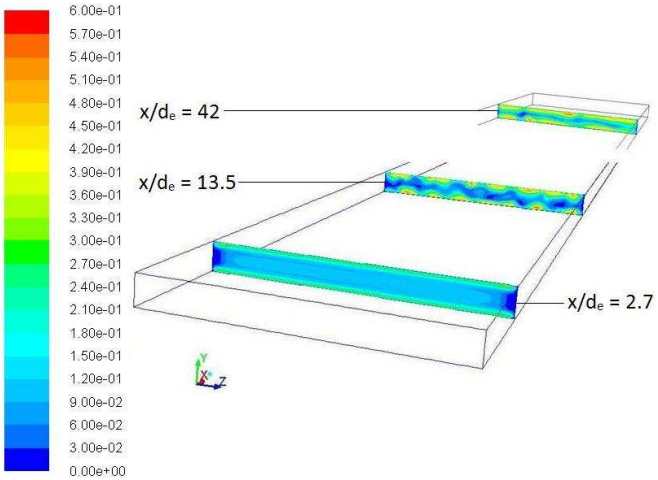

Figure 3 Flow structure at different x/d_e. Laminar modelling results for $Re_{in} = 1300$, $Gr_{qin} = 3.6 \cdot 10^8$

Flow structure at fixed z (**Figure 4**, **Figure 5**) and at y = h/2 (**Figure 6**, **Figure 7**) just confirms the previous information that at the very beginning of the heated part of the channel there are no vortexes, but they appear soon and remain in some part of the channel. This affects the velocity profile and it becomes distorted. So, as a result of vortex formation, the heat transfer is also increasing. The appearance of the circular flows in the channel influences the distribution of the temperature on the channel's walls and this directly affects the heat transfer distribution along the channel.

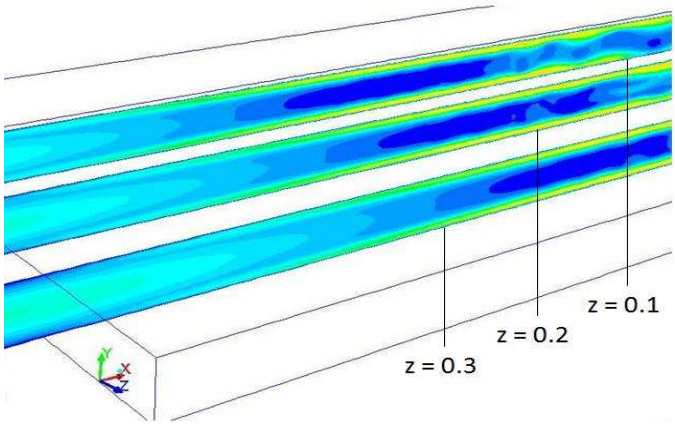

Figure 4 Flow structure for different z at the beginning ($x/d_e \approx 0 – 4$) of heated channel. Laminar modelling results for $Re_{in} = 1300$, $Gr_q = 3.6 \cdot 10^8$

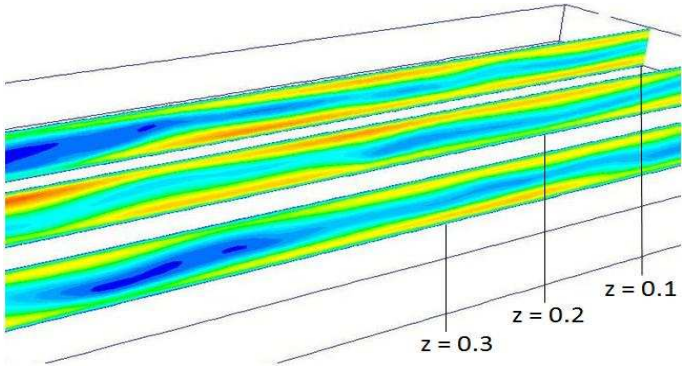

Figure 5 Flow structure for different z in the heat transfer stabilized region ($x/d_e \approx 40 – 47$) of heated channel. Laminar modelling results for $Re_{in} = 1300$, $Gr_q = 3.6 \cdot 10^8$

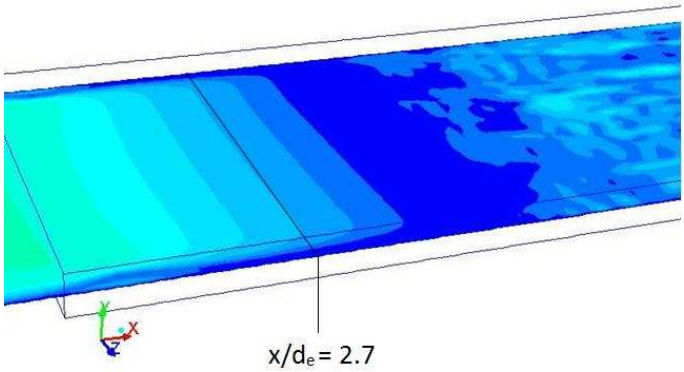

Figure 6 Flow structure for y = h/2 (in the centre) at the beginning ($x/d_e \approx 0 – 4$) of heated channel. Laminar modelling results for $Re_{in} = 1300$, $Gr_q = 3.6 \cdot 10^8$

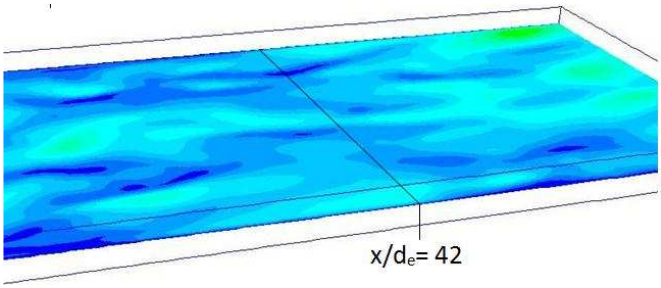

Figure 7 Flow structure for y = h/2 (in the centre) in the heat transfer stabilized region ($x/d_e \approx 40 - 47$) of heated channel. Laminar modelling results for $Re_{in} = 1300$, $Gr_q = 3.6 \cdot 10^8$

Variation of heat transfer along the channel for $Re_{in} = 1300$ using different models is illustrated in **Figure 8**.

As it can be seen from **Figure 8**a, till $x/d_e \leq 10$ the modelled three-dimensional heat transfer results (laminar model) coincide well with the experiment, but at $x/d_e > 10$ the experimental data are higher than numerical ones. From the beginning of the heated section, the two-dimensional modelling results (laminar model) give smaller Nu values than the experimental ones.

The used turbulence transition models do not improve prediction of the mixed convection heat transfer for $Re_{in} = 1300$ in comparison with laminar model. Transitional models show the same results.

At larger Re number ($Re_{in} = 2000$), the variation of heat transfer along the channel is similar to the case of smaller Re numbers, but the distance at which modelling results give smaller Nu numbers in comparison to the experimental data is different i.e. it happens at $x/d_e \approx 14$ (**Figure 9**a). Steady state two-dimensional results (laminar model) are still lower than the experimental ones practically from the beginning of the heated section.

Turbulence transition models show practically the same results as the laminar 3D model i.e. at $x/d_e \approx 14$ experimental data are higher than the numerical ones, except SST turbulence transition model which gives the best correlation with experimental data.

CONCLUSION

Analysis of the numerical modelling data on the aiding mixed convection in transition region in a vertical rectangular channel with symmetrical heating leads to the following conclusions:

1. The performed 2D and 3D numerical analysis has shown that vortexes exist in a vertical flat channel in the analyzed Re region.
2. 3D numerical modelling shows similar (symmetrical flow structure is observed) results to 2D modelling.
3. It has also been demonstrated that the best correlation of the numerical modelling results with the experimental heat transfer data is obtained with the laminar model for smaller analyzed Re numbers and with the SST transition model for higher Re numbers.

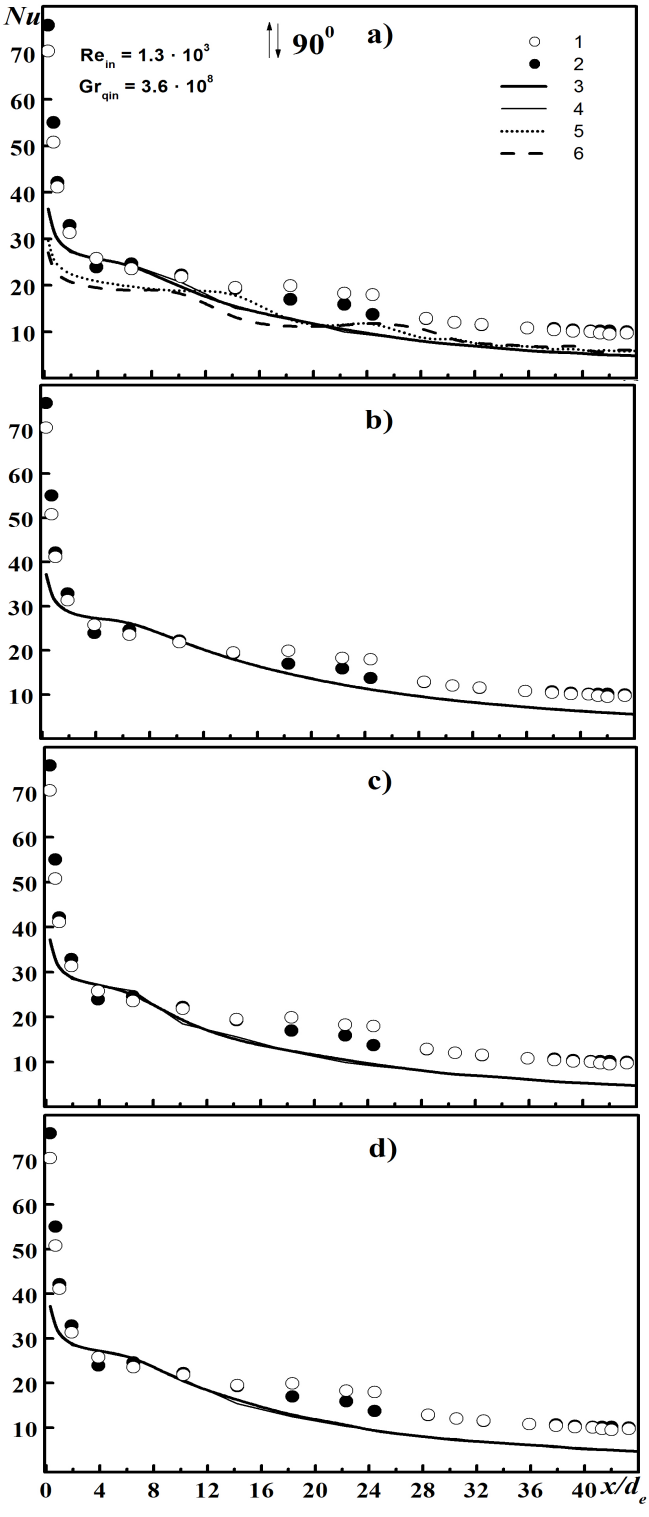

Figure 8 Variation of heat transfer along the channel. 1 – experimental data (1 wall); 2 – experimental data (2 wall); 3 – 3D numerical modelling results (1 wall); 4 – 3D numerical modelling results (2 wall); 5 – 2D numerical modelling results (1 wall); 6 – 2D numerical modelling results (2 wall). a) Laminar; b) SST; c) kkl-ω; d) Re Stress ω models

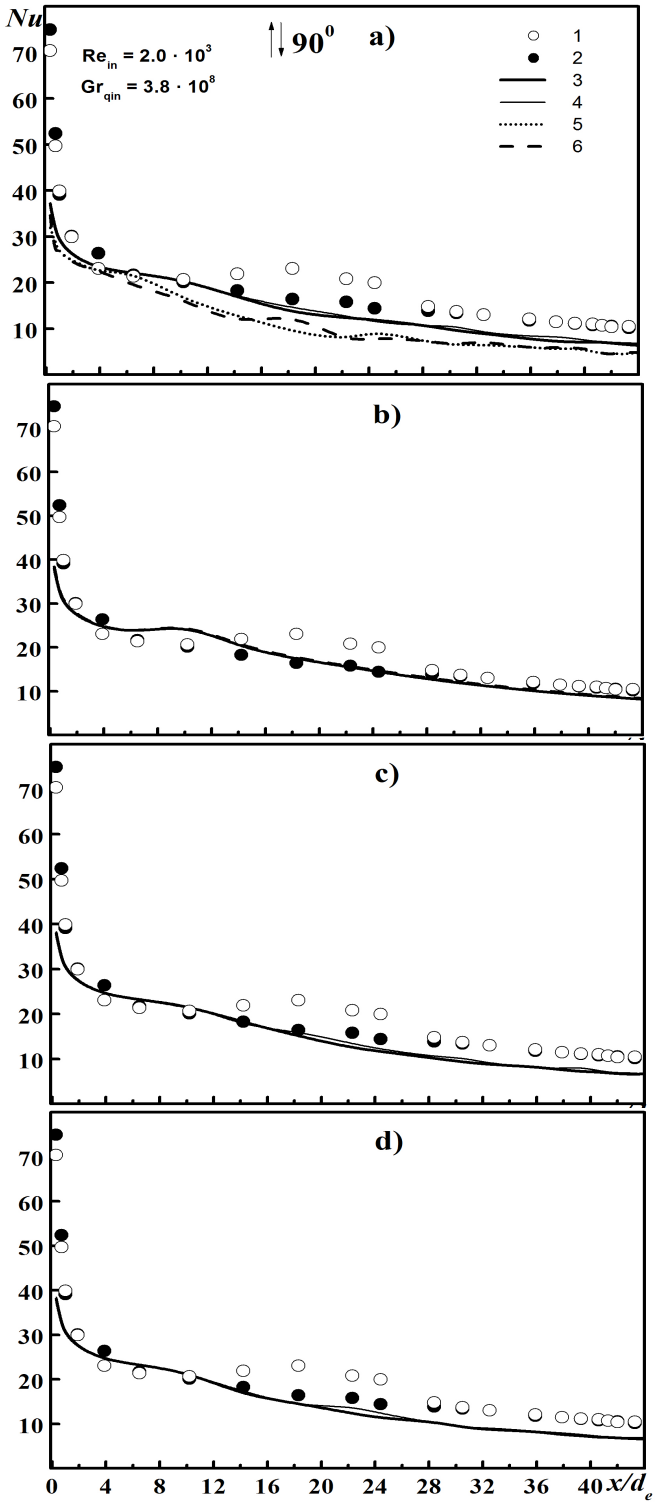

Figure 9 Variation of heat transfer along the channel. 1 – experimental data (1 wall); 2 – experimental data (2 wall); 3 – 3D numerical modelling results (1 wall); 4 – 3D numerical modelling results (2 wall); 5 – 2D numerical modelling results (1 wall); 6 – 2D numerical modelling results (2 wall). a) Laminar; b) SST; c) kkl-ω; d) Re Stress ω models

REFERENCES

[1] Petukhov B. S., Polyakov A. F., and Strigin B. K., *Heat transfer investigations in tubes under viscous-gravitational flow*, Energija, Moscow, Vol. 1, 1968.

[2] Jackson J. D., Cotton M. A., and Axell B. P., Studies of mixed convection in vertical tubes. Review, *International Journal of Heat Fluid Flow*, Vol. 10, No. 1, 1988, pp. 2-15.

[3] Jackson J. D., Influences of buoyancy on velocity, turbulence and heat transfer in ascending and descending flows in vertical passages, *Proceedings of the 4th Baltic Heat Transfer Conference. Advances in Heat Transfer Engineering*, Kaunas, Lithuania, August 2003, pp. 57-78.

[4] Vilemas J., and Poškas P., *Effect of body forces on turbulent heat transfer in channels*, LEI-Bigell House, Kaunas-New York, 1999.

[5] Scheele G. F., Rosen E. M., and Hanratty T. J.. Effects of Natural Convection on Transition to Turbulence in Vertical Pipes, *Canadian Journal of Chemical Engineering*, Vol. 38, 1960, pp. 67-73.

[6] Scheele G. F., and Hanratty T. J., Effects of Natural Convection Instabilities on Rates of Heat Transfer at Low Reynolds Numbers, *AIChE J.*, Vol. 9, No. 2, 1963, pp. 183-185.

[7] Petukhov B. S., Polyakov A. F., and Strigin B. K., *Heat Transfer Investigations in Tubes Under Viscous-Gravitational Flow*, Energija, Moscow, Vol. 1, 1968, (in Russian).

[8] Petukhov B. S., Genin L. G., and Kovalev S. A., *Heat Transfer in Nuclear Installations*, Energoatomizdat, Moscow, 1986 (in Russian).

[9] Joye D. D., and Jacobs W. S., Backflow in the Inlet Region of Opposing Mixed Convection Heat Transfer in a Vertical Tube, *Proceedings of the 10th International Heat Transfer Conference*, Vol. 5, 1994, pp. 489-494.

[10] Behzadmehr A., Laneville A., and Galanis N., Experimental Study of Onset of Laminar-Turbulent Transition in Mixed Convection in a Vertical Heated Tube, *International Journal of Heat and Mass Transfer*, Vol. 51, No. 25-26, 2008, pp. 5895–5905.

[11] Poskas P., Poskas R., Sirvydas A., and Smaizys A., Experimental investigation of opposing mixed convection heat transfer in the vertical flat channel in a laminar-turbulent transition region, *International Journal of Heat and Mass Transfer*, Vol. 54, No. 1-3, 2011, pp. 662-668.

[12] Walters D. K., and Cokljat D., A three-equation eddy-viscosity model for Reynolds-averaged Navier-Stokes simulations of transitional flows, *Journal of Fluids Engineering*, Vol. 130, 2008.

[13] Menter F. R., Langtry R. B., Likki S. R., Suzen Y. B., Huang P. G., and Volker S., A correlation based transition model using local variables. Part 1. Model formulation, *Journal of Turbomachinery*, Vol. 128, No. 3, 2004, pp. 413-422.

[14] Menter F. R., Two-equation eddy-viscosity turbulence models for engineering applications, *AIAA Journal*, Vol. 32, No. 8, 1994, pp. 1598-1605.

[15] Wilcox D. C., *Turbulence modelling for CFD*. DCW Industries, Inc., La Canada, California, 1998.

[16] Lauder B. E., Reece G. J., and Rodi W., Progress in the development of a Reynolds-Stress turbulence closure, *Journal of Fluid Mechanics*, Vol. 68, No. 3, 1975, pp. 537-566.

[17] ANSYS-FLUENT Inc., 2009. FLUENT 12.0 User Documentation.